18. Phillips A, Tang JL (1972) The effect of loading path on the yield surface at elevated temperatures. Int J Solids Struct 8:463–474
19. Abu Al-Rub RK, Voyiadjis GZ (2003) On the coupling of anisotropic damage and plasticity models for ductile materials. Int J Solids Struct 40:2611–2643

Nonlinear 2D Wing Models

► Aerothermoelastic Behavior of Lifting Surfaces
► Aerothermoelastic Control of Lifting Surfaces

Nonlinear Aerothermoelastic Analysis

► Aerothermoelastic Behavior of Flat and Curved Panels
► Aerothermoelastic Behavior of Lifting Surfaces

Nonlinear Aerothermoelastic Control Analysis

► Aerothermoelastic Control of Lifting Surfaces

Nonlinear Fracture Models of Magnetoelectroelastic Media

CuiYing Fan[1], MingHao Zhao[1] and Ernian Pan[1,2]
[1]Henan Key Engineering Laboratory for Anti-fatigue Manufacturing Technology and the School of Mechanical Engineering, Zhengzhou University, Zhengzhou, People's Republic of China
[2]Department of Civil Engineering, Computer Modeling and Simulation Group, University of Akron, Akron, OH, USA

Overview

Piezoelectric and magnetoelectroelastic materials have been widely used in smart devices and structures. Fracture mechanics of these materials have attracted extensive studies [1–3]. Remarkable discrepancies between theory and experiment were observed. Early theoretical studies on fracture of piezoceramics showed that the applied electric field inhibits crack propagation irrespective of its sign [4], while the experiments by Park and Sun [5] demonstrated that the failure stresses decrease with increasing applied positive electric field but increase with increasing magnitude of the applied negative electric field.

Based on Dugdale model [6], Gao et al. [7] proposed the strip polarization saturation (PS) model for explaining the observed experimental results and studying the nonlinear fracture behavior of piezoelectric media. In the PS model, the electric displacement reaches the saturation value in the electric yielding zone. From the energy point of view, McMeeking [8] pointed out that the electric displacement would behave like the strain, and the electric field strength like the mechanical strength. Later, Zhang et al. [9] proposed the dielectric breakdown (DB) model for the nonlinear fracture in piezoelectric media, in which the electric field reaches the critical value in the yielding strip.

Considering the electric and magnetic yielding near the crack tip, Zhao and Fan [10] and Fan and Zhao [11] proposed the strip electric-magnetic breakdown (SEMB) and strip electric-magnetic polarization saturation (SEMPS) models to study the nonlinear effect of the electric and magnetic fields on the fracture of magnetoelectroelastic (MEE) materials.

Although the PS or SEMPS model and DB or SEMB model were established based on two different physical points of view, they surprisingly predict the same results on the fracture for a crack in an infinite or a finite piezoelectric and magnetoelectroelastic medium [11, 12].

Stroh Formalism

For the two-dimensional deformation in the x_1-x_2 plane, in which the extended displacement vector

$\mathbf{u} = \begin{pmatrix} u_1 & u_2 & u_3 & \varphi & \psi \end{pmatrix}^T$ and the extended stress function vector $\mathbf{\Phi} = \begin{pmatrix} \phi_1 & \phi_2 & \phi_3 & \phi_4 & \phi_5 \end{pmatrix}^{\mathrm{T}}$ depend only on x_1 and x_2, the general solution takes the form

$$\mathbf{u} = \mathbf{A}\mathbf{f}(z) + \bar{\mathbf{A}}\overline{\mathbf{f}(z)} \tag{1}$$

$$\mathbf{\Phi} = \mathbf{B}\mathbf{f}(z) + \overline{\mathbf{B}}\overline{\mathbf{f}(z)} \tag{2}$$

where $\mathbf{A} = (\mathbf{a}_1 \ \ \mathbf{a}_2 \ \ \mathbf{a}_3 \ \ \mathbf{a}_4 \ \ \mathbf{a}_5)$ and $\mathbf{B} = (\mathbf{b}_1 \ \ \mathbf{b}_2 \ \ \mathbf{b}_3 \ \ \mathbf{b}_4 \ \ \mathbf{b}_5)$ are the eigenvectors, $\mathbf{f}(\mathrm{z}) = \begin{pmatrix} \mathrm{f}_1(\mathrm{z}_1) & \mathrm{f}_2(\mathrm{z}_2) & \mathrm{f}_3(\mathrm{z}_3) & \mathrm{f}_4(\mathrm{z}_4) & \mathrm{f}_5(\mathrm{z}_5) \end{pmatrix}^{\mathrm{T}}$ is an analytic function vector, $z_\alpha = x_1 + p_\alpha x_2$, and p_α is a complex eigenvalue with a positive imaginary part. While the extended stress function vector $\mathbf{\Phi}$ is related to the extended stresses by

$$\Sigma_2 = (\sigma_{21} \quad \sigma_{22} \quad \sigma_{23} \quad D_2 \quad B_2)^T = \mathbf{\Phi}_{,1} \tag{3a}$$

$$\Sigma_1 = (\sigma_{11} \quad \sigma_{12} \quad \sigma_{13} \quad D_1 \quad B_1)^T = -\mathbf{\Phi}_{,2} \tag{3b}$$

the eigenvalue p_α is determined by the following standard eigenequations [2]:

$$\begin{pmatrix} \mathbf{N}_1 & \mathbf{N}_2 \\ \mathbf{N}_3 & \mathbf{N}_1^T \end{pmatrix} \begin{pmatrix} \mathbf{a} \\ \mathbf{b} \end{pmatrix} = p \begin{pmatrix} \mathbf{a} \\ \mathbf{b} \end{pmatrix} \tag{4}$$

where $\mathbf{N}_1 = -\mathbf{T}^{-1}\mathbf{R}^T$, $\mathbf{N}_2 = \mathbf{T}^{-1} = \mathbf{N}_2^T$, $\mathbf{N}_3 = \mathbf{R}\mathbf{T}^{-1}\mathbf{R}^T - \mathbf{Q} = \mathbf{N}_3^T$, and $\mathbf{Q} = \begin{pmatrix} c_{i1k1} & e_{11i} & f_{11i} \\ e_{11i}^T & -\kappa_{11} & -g_{11} \\ f_{11i}^T & -g_{11} & -\mu_{11} \end{pmatrix}$, $\mathbf{R} = \begin{pmatrix} c_{i1k2} & e_{21i} & f_{21i} \\ e_{12i}^T & -\kappa_{12} & -g_{12} \\ f_{12i}^T & -g_{12} & -\varpi_{12} \end{pmatrix}$, $\mathbf{T} = \begin{pmatrix} c_{i2k2} & e_{22i} & f_{22i} \\ e_{22i}^T & -\kappa_{22} & -g_{22} \\ f_{22i}^T & -g_{22} & -\mu_{22} \end{pmatrix}$, where $i, k = 1, 2, 3$. It is noted that matrices $\mathbf{A}$ and $\mathbf{B}$ have the following relationship:

$$\begin{aligned} \mathbf{A}\mathbf{A}^{\mathrm{T}} + \overline{\mathbf{A}\mathbf{A}^{\mathrm{T}}} &= \mathbf{B}\mathbf{B}^{\mathrm{T}} + \overline{\mathbf{B}\mathbf{B}^{\mathrm{T}}} = \mathbf{0} \\ \mathbf{B}\mathbf{A}^{\mathrm{T}} + \overline{\mathbf{B}\mathbf{A}} &= \mathbf{A}\mathbf{B}^{\mathrm{T}} + \overline{\mathbf{A}\mathbf{B}^{\mathrm{T}}} = \mathbf{I} \end{aligned} \tag{5}$$

where $\mathbf{I}$ is a 5×5 unit matrix. In addition, the following important matrix $\mathbf{H}$ is introduced [10]:

$$\mathbf{H} = 2\mathrm{Re}[\mathrm{i}\mathbf{A}\mathbf{B}^{-1}], \qquad \mathbf{H}^{-1} = \begin{pmatrix} \mathbf{F}_1 & \mathbf{F}_2^{\mathrm{T}} & \mathbf{F}_3^{\mathrm{T}} \\ \mathbf{F}_2 & F_{44} & F_{45} \\ \mathbf{F}_3 & F_{54} & F_{55} \end{pmatrix} \tag{6}$$

The following quantities, which will be used later, are defined as:

$$\begin{aligned} \mathbf{F}_1 &= \begin{pmatrix} F_{11} & F_{12} & F_{13} \\ F_{21} & F_{22} & F_{23} \\ F_{31} & F_{32} & F_{33} \end{pmatrix} \\ \mathbf{F}_2 &= \begin{pmatrix} F_{41} & F_{42} & F_{43} \end{pmatrix} \\ \mathbf{F}_2 &= \begin{pmatrix} F_{51} & F_{52} & F_{53} \end{pmatrix} \end{aligned} \tag{7a}$$

and

$$\begin{aligned} (\mathbf{G}_{11})_l &= -\frac{1}{2i}\left(\mathbf{A}\langle p_\alpha\rangle\mathbf{B}^{\mathrm{T}} - \bar{\mathbf{A}}\langle \bar{p}_\alpha\rangle\bar{\mathbf{B}}^{\mathrm{T}}\right)_{4l} \\ (\mathbf{G}_{12})_l &= -\frac{1}{2i}\left(\mathbf{A}\langle p_\alpha\rangle\mathbf{B}^{\mathrm{T}} - \bar{\mathbf{A}}\langle \bar{p}_\alpha\rangle\bar{\mathbf{B}}^{\mathrm{T}}\right)_{5l} \\ G_{21} &= -\frac{1}{2i}\left(\mathbf{A}\langle p_\alpha\rangle\mathbf{B}^{\mathrm{T}} - \bar{\mathbf{A}}\langle \bar{p}_\alpha\rangle\bar{\mathbf{B}}^{\mathrm{T}}\right)_{44} \\ G_{22} &= -\frac{1}{2i}\left(\mathbf{A}\langle p_\alpha\rangle\mathbf{B}^{\mathrm{T}} - \bar{\mathbf{A}}\langle \bar{p}_\alpha\rangle\bar{\mathbf{B}}^{\mathrm{T}}\right)_{54} \\ G_{31} &= -\frac{1}{2i}\left(\mathbf{A}\langle p_\alpha\rangle\mathbf{B}^{\mathrm{T}} - \bar{\mathbf{A}}\langle \bar{p}_\alpha\rangle\bar{\mathbf{B}}^{\mathrm{T}}\right)_{45} \\ G_{32} &= -\frac{1}{2i}\left(\mathbf{A}\langle p_\alpha\rangle\mathbf{B}^{\mathrm{T}} - \bar{\mathbf{A}}\langle \bar{p}_\alpha\rangle\bar{\mathbf{B}}^{\mathrm{T}}\right)_{55} \end{aligned} \tag{7b}$$

and F_{ij} and G_{ij} are material related constants.

Strip Electric-magnetic Polarization Saturation (SEMPS) Model

To consider the saturation of electric displacement and the magnetic induction, the strip

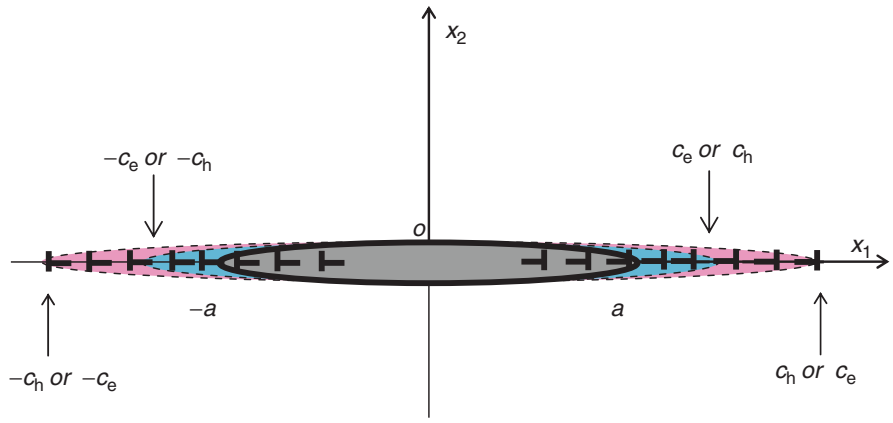

Nonlinear Fracture Models of Magnetoelectroelastic Media, Fig. 1 Schematic distribution of extended dislocation arrays in a magnetoelectroelastic medium

electric-magnetic polarization saturation (SEMPS) model is developed where the nonlinear behavior of cracks under combined mechanical-electric-magnetic loadings in MEE media can be studied. In this model, the material is assumed to be mechanically brittle, and electrically and magnetically ductile. In this section, a crack in an infinite body under uniformly applied mechanical-electric-magnetic loadings at infinity is taken as an example to present the basic features of the SEMPS model. The electric and magnetic yielding zones are the two strips in fronts of the crack, i.e., the segments $(-c_e, -a)$ and (a, c_e) for the electric yielding strips and $(-c_h, -a)$ and (a, c_h) for the magnetic yielding strips, as schematically shown in Fig. 1. The real crack is $(-a,\ a)$. It is noted that in the electric yielding strip, the electric displacement equals the electric displacement saturation, and in the magnetic yielding strip, the magnetic induction equals the magnetic induction saturation. Thus, the electric crack extends over the segment $(-c_e, c_e)$, and the magnetic crack over $(-c_h, c_h)$. A crack can be simulated by continuously distributed dislocations: elastic dislocations from $-a$ to a, electric dislocations from $-c_e$ to c_e [9], and magnetic dislocations from $-c_h$ to c_h [10].

The boundary conditions along the crack faces and the electric and magnetic yielding strips for an electrically and magnetically impermeable crack are

$$\Sigma_2 = \left(\sigma_{21}\ \ \sigma_{22}\ \ \sigma_{23}\ \ D_2\ \ B_2\right)^T = 0, \qquad |x_1| \le a \tag{8a}$$

$$\begin{aligned} &u_i(x_1,0^+) = u_i(x_1,0^-), \quad i = 1,2,3, \\ &D_2(x_1,0^+) = D_2(x_1,0^-) = D_S, \qquad a < |x_1| < c_e, \\ &B_2(x_1,0^+) = B_2(x_1,0^-) = B_S, \qquad a < |x_1| < c_h \end{aligned} \tag{8b}$$

where superscript "+" ("−") denotes the quantities on the upper (lower) crack faces, and D_S and B_S are, respectively, the electric displacement saturation and the magnetic induction saturation.

Dual Boundary Integral Equations of the SEMPS Model

We introduce five distribution functions, $g_i(x_1)$, that are corresponding to the Burgers vector components, $\mathbf{b}^* = \left(b_1\ \ b_2\ \ b_2\right)^T$, the electric potential discontinuity, $\Delta\varphi$, and the magnetic potential discontinuity, $\Delta\psi$, such that $g_i(x_1)\, b_i\, dx_1$ (where $b_4 \equiv \Delta\varphi$ and $b_5 \equiv \Delta\psi$) represents the strength of the extended Burgers vector located at x_1 in the interval dx_1. Thus, using Green's functions expressed by the extended dislocation, as given in [10] and the boundary conditions in (8), we have the following extended dual integral equations of the SEMPS model [11]:

$$\int_{-a}^{a} \frac{1}{\pi(x_1 - x_1')} \mathbf{F}_1 \langle g_i \rangle \mathbf{b}^* dx_1' + \int_{-c_e}^{c_e} \frac{1}{\pi(x_1 - x_1')} \mathbf{F}_2^T g_4 \Delta\varphi dx_1' + \int_{-c_h}^{c_h} \frac{1}{\pi(x_1 - x_1')} \mathbf{F}_3^T g_5 \Delta\psi dx_1' + \mathbf{t}^* = 0, \quad |x_1| \le a \tag{9a}$$

$$\int_{-a}^{a} \frac{1}{\pi(x_1 - x_1')} \mathbf{F}_2 \langle g_i \rangle \mathbf{b}^* dx_1' + \int_{-c_e}^{c_e} \frac{1}{\pi(x_1 - x_1')} F_{44} g_4 \Delta\varphi dx_1' + \int_{-c_h}^{c_h} \frac{1}{\pi(x_1 - x_1')} F_{45} g_5 \Delta\psi dx_1' + D_2^\infty = 0, \quad |x_1| \le a \tag{9b}$$

$$\int_{-a}^{a} \frac{1}{\pi(x_1 - x_1')} \mathbf{F}_3 \langle g_i \rangle \mathbf{b}^* dx_1' + \int_{-c_e}^{c_e} \frac{1}{\pi(x_1 - x_1')} F_{54} g_4 \Delta\varphi dx_1' + \int_{-c_h}^{c_h} \frac{1}{\pi(x_1 - x_1')} F_{55} g_5 \Delta\psi dx_1' + B_2^\infty = 0, \quad |x_1| \le a \tag{9c}$$

$$\int_{-a}^{a} \frac{1}{\pi(x_1 - x_1')} \mathbf{F}_2 \langle g_i \rangle \mathbf{b}^* dx_1' + \int_{-c_e}^{c_e} \frac{1}{\pi(x_1 - x_1')} F_{44} g_4 \Delta\varphi dx_1' + \int_{-c_h}^{c_h} \frac{1}{\pi(x_1 - x_1')} F_{45} g_5 \Delta\psi dx_1' + D_2^\infty = D_S, \quad a \le |x_1| \le c_e \tag{9d}$$

$$\int_{-a}^{a} \frac{1}{\pi(x_1 - x_1')} \mathbf{F}_3 \langle g_i \rangle \mathbf{b}^* dx_1' + \int_{-c_e}^{c_e} \frac{1}{\pi(x_1 - x_1')} F_{54} g_4 \Delta\varphi dx_1' + \int_{-c_h}^{c_h} \frac{1}{\pi(x_1 - x_1')} F_{55} g_5 \Delta\psi dx_1' + B_2^\infty = B_S, \quad a \le |x_1| \le c_h \tag{9e}$$

where $\langle g_i(x_1) \rangle$ is a 3×3 diagonal matrix and

$$\begin{aligned} \mathbf{t} &= \begin{pmatrix} \sigma_{12}^\infty & \sigma_{22}^\infty & \sigma_{32}^\infty & D_2^\infty & B_2^\infty \end{pmatrix}^T \\ &= \begin{pmatrix} \mathbf{t}^{*T} & D_2^\infty & B_2^\infty \end{pmatrix}^T \\ \mathbf{t}^* &= \begin{pmatrix} \sigma_{12}^\infty & \sigma_{22}^\infty & \sigma_{32}^\infty \end{pmatrix}^T \end{aligned} \tag{10}$$

Equation (9) is an extension of the classical Cauchy-type dual integral equations in elastic fracture mechanics to the MEE material.

Analytical Solution of the SEMPS Model

From (9a)–(9c), the distribution functions $g_i(x_1)$ can be solved

$$\langle g_i(x_1) \rangle \mathbf{b}^* = \mathbf{F}_1^{*-1} \mathbf{T}^* \frac{x_1}{\left(a^2 - x_1^2\right)^{1/2}}, \qquad |x_1| \le a \tag{11}$$

where

$$\begin{aligned} \mathbf{F}_1^* &= \mathbf{F}_1 + [\mathbf{F}_2^{\mathrm{T}}(\mathbf{F}_3 F_{45} - \mathbf{F}_2 F_{55}) \\ &\quad + \mathbf{F}_3^{\mathrm{T}}(\mathbf{F}_2 F_{54} - \mathbf{F}_3 F_{44})]/(F_{55}F_{44} - F_{54}F_{45}) \\ \mathbf{T}^* &= \mathbf{t}^* + [(F_{54}\mathbf{F}_3^{\mathrm{T}} - F_{55}\mathbf{F}_2^{\mathrm{T}})D_2^\infty \\ &\quad + (F_{45}\mathbf{F}_2^{\mathrm{T}} - F_{44}\mathbf{F}_3^{\mathrm{T}})B_2^\infty]/(F_{55}F_{44} - F_{54}F_{45}) \end{aligned} \tag{12}$$

Solving Eq. (9) requires the relative size of the electric yielding zone and the magnetic yielding zone, namely, $a \le c_e \le c_h$ or $a \le c_h \le c_e$. However, c_e and c_h are actually the two key

parameters to be determined in the SEMPS model. Therefore, we discuss the following two different cases separately.

If the magnetic yielding zone is longer than the electric yielding zone ($a \le c_e \le c_h$), we have

$$g_5\Delta\psi = \begin{cases} \dfrac{B_S}{F_{55}\pi}\left[\mathrm{ch}^{-1}\left|\dfrac{c_h^2 - \mathrm{a}x_1}{c_h(\mathrm{a}-x_1)}\right| - \mathrm{ch}^{-1}\left|\dfrac{c_h^2 + \mathrm{a}x_1}{c_h(\mathrm{a}+x_1)}\right|\right] - \dfrac{F_{54}}{F_{55}}g_4\Delta\varphi - \dfrac{\mathbf{F}_3}{F_{55}}\langle g_i\rangle\mathbf{b}^*, & |x_1| \le a, \\ \dfrac{B_S}{F_{55}\pi}\left[\mathrm{ch}^{-1}\left|\dfrac{c_h^2 - \mathrm{a}x_1}{c_h(\mathrm{a}-x_1)}\right| - \mathrm{ch}^{-1}\left|\dfrac{c_h^2 + \mathrm{a}x_1}{c_h(\mathrm{a}+x_1)}\right|\right] - \dfrac{F_{54}}{F_{55}}g_4\Delta\varphi, & a \le |x_1| \le c_e, \\ \dfrac{B_S}{F_{55}\pi}\left[\mathrm{ch}^{-1}\left|\dfrac{c_h^2 - \mathrm{a}x_1}{c_h(\mathrm{a}-x_1)}\right| - \mathrm{ch}^{-1}\left|\dfrac{c_h^2 + \mathrm{a}x_1}{c_h(\mathrm{a}+x_1)}\right|\right], & c_e \le |x_1| \le c_h \end{cases} \tag{13a}$$

$$g_4\Delta\varphi = \begin{cases} \dfrac{D_S^*}{G_2\pi}\left[\mathrm{ch}^{-1}\left|\dfrac{c_e^2 - ax_1}{c_e(a-x_1)}\right| - \mathrm{ch}^{-1}\left|\dfrac{c_e^2 + ax_1}{c_e(a+x_1)}\right|\right] - \dfrac{\mathbf{G}_1}{G_2}\mathbf{F}_1^{*-1}\mathbf{T}^*\dfrac{x_1}{\left(a^2 - x_1^2\right)^{1/2}}, & |x_1| \le a, \\ \dfrac{D_S^*}{G_2\pi}\left[\mathrm{ch}^{-1}\left|\dfrac{c_e^2 - ax_1}{c_e(a-x_1)}\right| - \mathrm{ch}^{-1}\left|\dfrac{c_e^2 + ax_1}{c_e(a+x_1)}\right|\right], & a \le |x_1| \le c_e \end{cases} \tag{13b}$$

where

$$\begin{aligned} &\mathbf{G}_1 = \mathbf{F}_3F_{45} - \mathbf{F}_2F_{55}, \quad G_2 = (F_{45}F_{54} - F_{44}F_{55}) \\ &D_S^* = F_{45}B_S - F_{55}D_S \end{aligned} \tag{14}$$

If the electric yielding zone is longer than the magnetic yielding zone ($a \le c_h \le c_e$), we have

$$g_4\Delta\varphi = \begin{cases} \dfrac{D_S}{F_{44}\pi}\left[\mathrm{ch}^{-1}\left|\dfrac{c_e^2 - ax_1}{c_e(a-x_1)}\right| - \mathrm{ch}^{-1}\left|\dfrac{c_e^2 + ax_1}{c_e(a+x_1)}\right|\right] - \dfrac{F_{45}}{F_{44}}g_5\Delta\psi - \dfrac{\mathbf{F}_2}{F_{44}}\langle g_i\rangle\mathbf{b}^*, & |x_1| \le a, \\ \dfrac{D_S}{F_{44}\pi}\left[\mathrm{ch}^{-1}\left|\dfrac{c_e^2 - ax_1}{c_e(a-x_1)}\right| - \mathrm{ch}^{-1}\left|\dfrac{c_e^2 + ax_1}{c_e(a+x_1)}\right|\right] - \dfrac{F_{45}}{F_{44}}g_5\Delta\psi, & a \le |x_1| \le c_h, \\ \dfrac{D_S}{F_{44}\pi}\left[\mathrm{ch}^{-1}\left|\dfrac{c_e^2 - ax_1}{c_e(a-x_1)}\right| - \mathrm{ch}^{-1}\left|\dfrac{c_e^2 + ax_1}{c_e(a+x_1)}\right|\right], & c_h \le |x_1| \le c_e \end{cases} \tag{15a}$$

$$g_5\Delta\psi = \begin{cases} \dfrac{B_S^*}{G_2\pi}\left[\mathrm{ch}^{-1}\left|\dfrac{c_h^2 - ax_1}{c_h(a-x_1)}\right| - \mathrm{ch}^{-1}\left|\dfrac{c_h^2 + ax_1}{c_h(a+x_1)}\right|\right] - \dfrac{\mathbf{G}_3}{G_2}\mathbf{F}_1^{*-1}\mathbf{T}^*\dfrac{x_1}{\left(a^2 - x_1^2\right)^{1/2}}, & |x_1| \le a, \\ \dfrac{B_S^*}{G_2\pi}\left[\mathrm{ch}^{-1}\left|\dfrac{c_h^2 - ax_1}{c_h(a-x_1)}\right| - \mathrm{ch}^{-1}\left|\dfrac{c_h^2 + ax_1}{c_h(a+x_1)}\right|\right], & a \le |x_1| \le c_h \end{cases} \tag{15b}$$

where

$$\mathbf{G}_3 = \mathbf{F}_2 F_{54} - \mathbf{F}_3 F_{44}, \quad B_S^* = F_{54} D_S - F_{44} B_S \tag{16}$$

To determine the sizes of the electric and magnetic yielding zones, the following two conditions should be supplemented: The electric displacement intensity factor, K_{Ds}, is zero at the end of the electric yielding zone and the magnetic induction intensity factor, K_{Bs}, is zero at the end of the magnetic yielding zone. With these, the sizes of the electric and magnetic yielding zones can be solved. When $a \le c_e \le c_h$, they are

$$\begin{aligned} R_e &= \frac{c_e - a}{a} = \sec\left(\frac{\pi D_2^*}{2D_S^*}\right) - 1 \\ R_h &= \frac{c_h - a}{a} = \sec\left(\frac{\pi B_2^\infty}{2B_S}\right) - 1 \end{aligned} \tag{17}$$

where

$$D_2^* = F_{45} B_2^\infty - F_{55} D_2^\infty \tag{18}$$

and when $a \le c_h \le c_e$, they are

$$\begin{aligned} R_e &= \frac{c_e - a}{a} = \sec\left(\frac{\pi D_2^\infty}{2D_S}\right) - 1 \\ R_h &= \frac{c_h - a}{a} = \sec\left(\frac{\pi B_2^*}{2B_S^*}\right) - 1 \end{aligned} \tag{19}$$

where

$$B_2^* = F_{54} D_2^\infty - F_{44} B_2^\infty \tag{20}$$

It is observed from these expressions that, for an impermeable crack, the sizes of the electric and magnetic yielding zones are related to the material properties, the applied loadings, the crack length, and the electric displacement saturation and the magnetic induction saturation.

Extended Intensity Factors and Local J-integral

Based on the sizes of electric and magnetic yielding zones, the extended stress ahead of the crack tip on the x_1-axis is expressed by the extended dislocation

$$\begin{aligned} \Sigma_2 &\equiv \left(\sigma_{12} \;\; \sigma_{22} \;\; \sigma_{32} \;\; D_2 \;\; B_2\right)^T \\ &= \int_{-a}^{a} \frac{1}{\pi(x_1 - x_1')} \begin{pmatrix} \mathbf{F}_1 \\ \mathbf{F}_2 \\ \mathbf{F}_3 \end{pmatrix} \langle g_i(x_1) \rangle \mathbf{b}^* dx_1' \\ &\quad + \int_{-c_e}^{c_e} \frac{1}{\pi(x_1 - x_1')} \begin{pmatrix} \mathbf{F}_2^T \\ F_{44} \\ F_{54} \end{pmatrix} g_4(x_1) \Delta\varphi dx_1' \\ &\quad + \int_{-c_h}^{c_h} \frac{1}{\pi(x_1 - x_1')} \begin{pmatrix} \mathbf{F}_3^T \\ F_{45} \\ F_{55} \end{pmatrix} g_5(x_1) \Delta\psi dx_1' + \mathbf{t} \end{aligned} \tag{21}$$

The extended local intensity factors for either $a \le c_e \le c_h$ or $a \le c_h \le c_e$ are then given by

$$\begin{aligned} \mathbf{K}^{(l)} &= \left(K_{II}^{(l)} \;\; K_I^{(l)} \;\; K_{III}^{(l)} \;\; K_D^{(l)} \;\; K_B^{(l)}\right)^T \\ &= \left(\mathbf{L} \;\; \mathbf{L}\mathbf{L}_D \;\; \mathbf{L}\mathbf{L}_B\right)\mathbf{K} \end{aligned} \tag{22}$$

where $\mathbf{L}$ is a 5×3 matrix and $\mathbf{L}_D$ and $\mathbf{L}_B$ are two column vectors. They are functions of the material property, given by

$$\begin{aligned} \mathbf{L} = \Bigg[&\begin{pmatrix} \mathbf{F}_1 \\ 0 \\ 0 \end{pmatrix} - \left(\begin{pmatrix} \mathbf{F}_2^T \\ 0 \\ 0 \end{pmatrix} - \frac{F_{54}}{F_{55}} \begin{pmatrix} \mathbf{F}_3^T \\ 0 \\ 0 \end{pmatrix} \right) \\ &\left(\frac{\mathbf{F}_2 F_{55} - \mathbf{F}_3 F_{45}}{F_{44} F_{55} - F_{54} F_{45}} \right) - \begin{pmatrix} \mathbf{F}_3^T \\ 0 \\ 0 \end{pmatrix} \frac{\mathbf{F}_3}{F_{55}} \Bigg] \mathbf{F}_1^{*-1} \end{aligned} \tag{23a}$$

$$\mathbf{L}_{\mathrm{D}} = (F_{54}\mathbf{F}_3^{\mathrm{T}} - F_{55}\mathbf{F}_2^{\mathrm{T}})/(F_{55}F_{44} - F_{54}F_{45})$$
$$\mathbf{L}_{\mathrm{B}} = (F_{45}\mathbf{F}_2^{\mathrm{T}} - F_{44}\mathbf{F}_3^{\mathrm{T}})/(F_{55}F_{44} - F_{54}F_{45}) \tag{23b}$$

In (22), the extended intensity factor $\mathbf{K}$ is defined as

$$\mathbf{K} = (K_{\mathrm{II}} \quad K_{\mathrm{I}} \quad K_{\mathrm{III}} \quad K_{\mathrm{D}} \quad K_{\mathrm{B}})^{\mathrm{T}} = \sqrt{\pi a}(\sigma_{12}^{\infty} \quad \sigma_{22}^{\infty} \quad \sigma_{32}^{\infty} \quad D_2^{\infty} \quad B_2^{\infty})^{\mathrm{T}} \tag{23c}$$

For the MEE media, the relationship between the local J-integral and the extended intensity factor is

$$J^{(l)} = \mathbf{K}^{\mathrm{T}}(\mathbf{L} \quad \mathbf{LL}_{\mathrm{D}} \quad \mathbf{LL}_{\mathrm{B}})^{\mathrm{T}}\frac{\mathbf{H}}{4}(\mathbf{L} \quad \mathbf{LL}_{\mathrm{D}} \quad \mathbf{LL}_{\mathrm{B}})\mathbf{K} \tag{24}$$

Equations (22)–(24) demonstrate that the local J-integral is only related to the material property and the extended intensity factor, and is independent of the yielding parameters, such as the electric displacement saturation, the magnetic induction saturation, and the size of the electric and magnetic yielding zones.

Strip Electric-magnetic Breakdown (SEMB) Model

Based on the arguments by McMeeking [8] and the relationship between the PS and DB models, we introduce the "electric breakdown" and "magnetic breakdown" concepts, which result in the strip electric-magnetic breakdown (SEMB) model. As schematically shown in Fig. 1, in this model, the MEE material is mechanically brittle, and two regions – the electric breakdown (or yielding) region and the magnetic breakdown (or yielding) region – are assumed along the crack front line, where the electric field strength in the electric breakdown region is equal to the electric breakdown strength, E_b, while the magnetic field strength in the magnetic breakdown region is equal to the magnetic breakdown strength, H_b.

For an electrically and magnetically impermeable crack, the boundary conditions along the crack faces and the electric and magnetic yielding strips are

$$\Sigma_2 = (\sigma_{21} \quad \sigma_{22} \quad \sigma_{23} \quad D_2 \quad B_2)^{\mathrm{T}} = 0, \quad |x_1| \le a \tag{25a}$$

$$\begin{aligned} &u_i(x_1,0^+) = u_i(x_1,0^-) \\ &E_2(x_1,0^+) = E_2(x_1,0^-) = E_b, \quad a < |x_1| < c_e \\ &H_2(x_1,0^+) = H_2(x_1,0^-) = H_b, \quad a < |x_1| < c_h \end{aligned} \tag{25b}$$

Dual Boundary Integral Equations of the SEMB Model

Using Green's functions for the extended dislocations given by Zhao and Fan [10] and the boundary conditions in (25), we have the following extended dual boundary integral equations of the SEMB model [10]:

$$\begin{aligned} &\int_{-a}^{a} \frac{1}{\pi(x_1 - x_1')}\mathbf{F}_1\langle g_i\rangle \mathbf{b}^* dx_1' \\ &+ \int_{-c_e}^{c_e} \frac{1}{\pi(x_1 - x_1')}\mathbf{F}_2^T g_4 \Delta\varphi dx_1' \\ &+ \int_{-c_h}^{c_h} \frac{1}{\pi(x_1 - x_1')}\mathbf{F}_3^T g_5 \Delta\psi dx_1' + \mathbf{t}^* = 0, \\ &\qquad |x_1| \le a \end{aligned} \tag{26a}$$

$$\begin{aligned} &\int_{-a}^{a} \frac{1}{\pi(x_1 - x_1')}\mathbf{F}_2\langle g_i\rangle \mathbf{b}^* dx_1' \\ &+ \int_{-c_e}^{c_e} \frac{1}{\pi(x_1 - x_1')}F_{44} g_4 \Delta\varphi dx_1' \\ &+ \int_{-c_h}^{c_h} \frac{1}{\pi(x_1 - x_1')}F_{45} g_5 \Delta\psi dx_1' + D_2^{\infty} = 0, \\ &\qquad |x_1| \le a \end{aligned} \tag{26b}$$

$$\int_{-a}^{a} \frac{1}{\pi(x_1 - x_1')} \mathbf{F}_3 \langle g_i \rangle \mathbf{b}^* dx_1' + \int_{-c_e}^{c_e} \frac{1}{\pi(x_1 - x_1')} F_{54} g_4 \Delta\varphi dx_1' + \int_{-c_h}^{c_h} \frac{1}{\pi(x_1 - x_1')} F_{55} g_5 \Delta\psi dx_1' + B_2^{\infty} = 0, \quad |x_1| \le a \tag{26c}$$

$$\int_{-a}^{a} \frac{1}{\pi(x_1 - x_1')} \mathbf{G}_{11} \langle g_i \rangle \mathbf{b}^* dx_1' + \int_{-c_e}^{c_e} \frac{1}{\pi(x_1 - x_1')} G_{21} g_4 \Delta\varphi dx_1' + \int_{-c_h}^{c_h} \frac{1}{\pi(x_1 - x_1')} G_{31} g_5 \Delta\psi dx_1' + E_2^{\infty} = E_b, \quad a \le |x_1| \le c_e \tag{26d}$$

$$\int_{-a}^{a} \frac{1}{\pi(x_1 - x_1')} \mathbf{G}_{12} \langle g_i \rangle \mathbf{b}^* dx_1' + \int_{-c_e}^{c_e} \frac{1}{\pi(x_1 - x_1')} G_{22} g_4 \Delta\varphi dx_1' + \int_{-c_h}^{c_h} \frac{1}{\pi(x_1 - x_1')} G_{32} g_5 \Delta\psi dx_1' + H_2^{\infty} = H_b, \quad a \le |x_1| \le c_h \tag{26e}$$

Equations (26a)–(26c) are very similar to (9a)–(9c) of the SEMPS model. Therefore, the solution for the distribution functions $g_i(x_1)$ is the same as in (11).

For the SEMB model, the following are the two supplementary conditions : The electric field intensity factor, K_{Es}, is zero at the end of the electric yielding zone and the magnetic field intensity factor, K_{Hs}, is zero at the end of the magnetic yielding zone. If the magnetic yielding zone is longer than the electric yielding zone ($a \le c_{\mathrm{e}} \le c_{\mathrm{h}}$), the sizes of the electric and magnetic yielding zones are given by

$$r_{e1} = c_e - a = a \sec\left(\frac{\pi D_{21}^*}{2D_{b1}^*}\right) - a \tag{27a}$$

$$r_{h1} = c_h - a = a \sec\left(\frac{\pi B_{21}^*}{2B_{b1}^*}\right) - a \tag{27b}$$

where

$$\begin{aligned} D_{21}^* &= \mathbf{q}_1 \mathrm{T}^* + (F_{55} D_2^{\infty} - F_{45} B_2^{\infty}) \\ &\quad (G_{21} G_{32} - G_{22} G_{31}) / (F_{55} F_{44} - F_{54} F_{45}) \\ D_{b1}^* &= G_{32}(E_b - E_2^{\infty}) - G_{31}(H_b - H_2^{\infty}) + D_{21}^* \\ B_{b1}^* &= H_b - H_2^{\infty} + B_{21}^* \\ B_{21}^* &= \mathbf{q}_2 \mathbf{T}^* + G_{22} \frac{F_{55} D_2^{\infty} - F_{45} B_2^{\infty}}{F_{55} F_{44} - F_{54} F_{45}} \\ &\quad + G_{32} \frac{F_{44} B_2^{\infty} - F_{54} D_2^{\infty}}{F_{55} F_{44} - F_{54} F_{45}} \end{aligned} \tag{28a}$$

$$\begin{aligned} \mathbf{q}_1 &= \Big[(\mathbf{G}_{11} G_{32} - \mathrm{G}_{12} G_{31}) \\ &\quad + \frac{\mathbf{F}_3 F_{45} - \mathbf{F}_2 F_{55})(G_{21} G_{32} - G_{22} G_{31})}{(F_{55} F_{44} - F_{54} F_{45})} \Big] \mathbf{F}_1^{*-1} \\ \mathbf{q}_2 &= \Big[\mathrm{G}_{12} + \frac{G_{22}(\mathbf{F}_3 F_{45} - \mathbf{F}_2 F_{55})}{(F_{55} F_{44} - F_{54} F_{45})} \\ &\quad + \frac{G_{32}(\mathbf{F}_2 F_{54} - \mathbf{F}_3 F_{44})}{(F_{55} F_{44} - F_{54} F_{45})} \Big] \mathbf{F}_1^{*-1} \end{aligned} \tag{28b}$$

If the electric yielding zone is longer than the magnetic yielding zone ($a \le c_{\mathrm{e}} \le c_{\mathrm{h}}$), the sizes of the electric and magnetic yielding zones are given by

$$r_{e2} = c_e - a = a \sec\left(\frac{\pi D_{22}^*}{2D_{b2}^*}\right) - a \tag{29a}$$

$$r_{h2} = c_h - a = a \sec\left(\frac{\pi B_{22}^*}{2B_{b2}^*}\right) - a \tag{29b}$$

where

$$
\begin{aligned}
D_{22}^{*} &= \mathbf{q}_4\mathbf{T}^{*} + G_{21}\frac{F_{55}D_2^{\infty} - F_{45}B_2^{\infty}}{F_{55}F_{44} - F_{54}F_{45}} \\
&\quad + G_{31}\frac{F_{44}B_2^{\infty} - F_{54}D_2^{\infty}}{F_{55}F_{44} - F_{54}F_{45}} \\
D_{b2}^{*} &= E_b - E_2^{\infty} + D_{22}^{*} \\
B_{22}^{*} &= \mathbf{q}_3\mathbf{T}^{*} + (F_{44}B_2^{\infty} - F_{54}D_2^{\infty}) \\
&\quad \times (G_{31}G_{22} - G_{32}G_{21})/(F_{55}F_{44} - F_{54}F_{45}) \\
B_{b2}^{*} &= G_{22}(E_b - E_2^{\infty}) - G_{21}(H_b - H_2^{\infty}) + B_{22}^{*}
\end{aligned}
\tag{30a}
$$

$$
\begin{aligned}
\mathbf{q}_3 &= \Big[(\mathbf{G}_{11}G_{22} - \mathbf{G}_{12}G_{21}) \\
&\quad + \frac{(\mathbf{F}_2F_{54} - \mathbf{F}_3F_{44})(G_{31}G_{22} - G_{32}G_{21})}{(F_{55}F_{44} - F_{54}F_{45})}\Big]\mathbf{F}_1^{*-1} \\
\mathbf{q}_4 &= \Big[\mathbf{G}_{11} + \frac{G_{21}(\mathbf{F}_3F_{45} - \mathbf{F}_2F_{55})}{(F_{55}F_{44} - F_{54}F_{45})} \\
&\quad + \frac{G_{31}(\mathbf{F}_2F_{54} - \mathbf{F}_3F_{44})}{(F_{55}F_{44} - F_{54}F_{45})}\Big]\mathbf{F}_1^{*-1}
\end{aligned}
\tag{30b}
$$

Extended Intensity Factors and Local J-integral

The stress in front of the crack tip on the x_1-axis is calculated by

$$
\begin{aligned}
\Sigma_2 &\equiv (\sigma_{12} \quad \sigma_{22} \quad \sigma_{32} \quad D_2 \quad B_2)^T \\
&= \int_{-a}^{a} \frac{1}{\pi(x_1 - x_1')}\begin{pmatrix}\mathbf{F}_1\\ \mathbf{F}_2\\ \mathbf{F}_3\end{pmatrix}\langle g_i(x_1)\rangle \mathbf{b}^{*} dx_1' \\
&\quad + \int_{-c_e}^{c_e} \frac{1}{\pi(x_1 - x_1')}\begin{pmatrix}\mathbf{F}_2^{\mathrm{T}}\\ F_{44}\\ F_{54}\end{pmatrix} g_4(x_1)\Delta\varphi dx_1' \\
&\quad + \int_{-c_h}^{c_h} \frac{1}{\pi(x_1 - x_1')}\begin{pmatrix}\mathbf{F}_3^{\mathrm{T}}\\ F_{45}\\ F_{55}\end{pmatrix} g_5(x_1)\Delta\psi dx_1' + \mathbf{t}
\end{aligned}
\tag{31}
$$

The extended local intensity factor for either $a \le c_e \le c_h$ or $a \le c_h \le c_e$ can be expressed as

$$
\mathbf{K}^{(l)} = \begin{pmatrix}\mathbf{M} & \mathbf{M}\mathbf{M}_D & \mathbf{M}\mathbf{M}_B\end{pmatrix}\mathbf{K} \tag{32}
$$

where $\mathbf{K}$ is the extended intensity factor defined in (17), $\mathbf{M}$ is a 5×3 matrix, and $\mathbf{M}_D$ and $\mathbf{M}_B$ are two column vectors. They are related to the material property as

$$
\begin{aligned}
\mathbf{M} = \Bigg[&\begin{pmatrix}\mathbf{F}_1\\ \mathbf{F}_2\\ \mathbf{F}_3\end{pmatrix} - \left(\begin{pmatrix}\mathbf{F}_2^{\mathrm{T}}\\ F_{44}\\ F_{54}\end{pmatrix} - \frac{G_{22}}{G_{32}}\begin{pmatrix}\mathbf{F}_3^{\mathrm{T}}\\ F_{45}\\ F_{55}\end{pmatrix}\right) \\
&\left(\frac{\mathbf{G}_{11}G_{32} - \mathrm{G}_{12}G_{31}}{G_{21}G_{32} - G_{22}G_{31}}\right) - \begin{pmatrix}\mathbf{F}_3^{\mathrm{T}}\\ F_{45}\\ F_{55}\end{pmatrix}\frac{\mathrm{G}_{12}}{G_{32}}\Bigg]\mathbf{F}_1^{*-1}
\end{aligned}
\tag{33a}
$$

$$
\begin{aligned}
\mathbf{M}_{\mathrm{D}} &= (F_{54}\mathbf{F}_3^T - F_{55}\mathbf{F}_2^T)/(F_{55}F_{44} - F_{54}F_{45}) \\
\mathbf{M}_{\mathrm{B}} &= (F_{45}\mathbf{F}_2^T - F_{44}\mathbf{F}_3^T)/(F_{55}F_{44} - F_{54}F_{45})
\end{aligned}
\tag{33b}
$$

Finally, the local J-integral is obtained as

$$
\begin{aligned}
J^{(l)} = \mathbf{K}^T(\mathbf{M} \quad \mathbf{M}\mathbf{M}_D \quad \mathbf{M}\mathbf{M}_B)^{\mathrm{T}}\frac{\mathbf{H}}{4} \\
(\mathbf{M} \quad \mathbf{M}\mathbf{M}_D \quad \mathbf{M}\mathbf{M}_B)\mathbf{K}
\end{aligned}
\tag{34}
$$

For an impermeable crack, the local J-integral is related to the material coefficients and the extended intensity factors, but is independent of the electric and magnetic breakdown strength.

Concluding Remarks

The SEMPS and SEMB models are presented as the extension of the PS and DB models in piezoelectricity. The results demonstrate that the local J-integral increases with increasing electric and magnetic fields applied. This means that a positive electric or magnetic field would promote propagation of an impermeable crack, while the negative electric or magnetic field would retard crack propagation. The local J-integral can be used as a parameter to describe and predict the fracture behavior in MEE media under combined mechanical-electric-magnetic loadings.

It should be pointed out the theoretical analysis carried out should be verified by the experimental observation. To the best of the authors' knowledge, however, no experimental result on fracture in the MEE material is available so far.

Acknowledgments The work was supported by the National Natural Science Foundation of China (No. 11102186, No.11072221, No. 11272290), and the Construction Project of Key Laboratory in Henan Colleges.

References

1. Suo Z, Kuo CM, Barnett DM, Willis JR (1992) Fracture mechanics for piezoelectric ceramics. J Mech Phys Solids 40:739–765
2. Zhang T-Y, Zhao MH, Tong P (2002) Fracture of piezoelectric ceramics. Adv Appl Mech 38:147–289
3. Kuna M (2010) Fracture mechanics of piezoelectric materials – where are we right now? Eng Fract Mech 77:309–326
4. Pak YE, Tobin A (1993) On electric field effects in fracture of piezoelectric materials. Mech Electromagn Mater Struct Appl Mech Div 161:51–62
5. Park S, Sun CT (1995) Fracture criteria for piezoelectric materials. J Am Ceram Soc 78:1475–1480
6. Dugdale DS (1960) Yielding of steel sheets containing slits. J Mech Phys Solids 8:100–104
7. Gao HJ, Zhang TY, Tong P (1997) Local and global energy release rates for an electrically yielded crack in a piezoelectric ceramic. J Mech Phys Solids 45:491–510
8. McMeeking RM (2001) Towards a fracture mechanics for brittle piezoelectric and dieletric materials. Int J Fract 108:25–41
9. Zhang T-Y, Zhao MH, Cao CF (2005) The strip dielectric breakdown model. Int J Fract 132:311–327
10. Zhao MH, Fan CY (2008) Strip electric-magnetic breakdown model in magnetoelectroelastic medium. J Mech Phys Solids 56:3441–3458
11. Fan CY, Zhao MH (2011) Nonlinear fracture of 2D magnetoelectroelastic media: analytical and numerical solutions. Int J Solids Struct 48:2373–2382
12. Fan CY, Zhao MH, Zhou YH (2009) Numerical solution of polarization saturation/dielectric breakdown model in 2D finite piezoelectric media. J Mech Phys Solids 57:1527–1544

Nonlinear Theory

► Continuous Dependence Results
► Nonlinear Thermoelastic Model
► Uniqueness and Continuous Dependence Results in Nonlinear Thermoviscoelasticity

Nonlinear Thermoelastic Model

Cătălin Galeş
Department of Mathematics, Faculty of Mathematics, "Al. I. Cuza" University of Iaşi, Iaşi, Romania

Synonyms

Thermoelasticity, Nonlinear theory

Overview

The theory of thermoelasticity studies the deformation of elastic continuums under the influence of mechanical forces and thermal changes. The origin of the theory of thermoelasticity goes back to the nineteenth century when the coupling between thermal and strain fields has been investigated for the first time (see [1, 2] for detailed historical notes concerning the development of the theory). Since its inception, during almost 200 years, many research studies have been dedicated to solve various practical and theoretical problems and to propose new thermoelastic models. The state of the art in thermoelasticity, including its generalized models and the related results, is described in various monographs [1–7].

Here, the classical theory of thermoelasticity is considered. The basic equations of the nonlinear thermoelasticity are presented in a self-contained manner. Thus, after a short section in which some aspects related to deformation and strain are recalled, the basic principles of mechanics and thermodynamics are formulated, and their local forms are derived. Then, the constitutive equations of a thermoelastic body are presented, and the consequences implied by the axioms of the constitutive theory are discussed. The restrictions imposed by the second law of thermodynamics are also analyzed. Finally, the basic equations of the nonlinear thermoelasticity are summarized.